Schwarz, U., Luhrmann, R., and Gassen, H. G. (1974), *Biochem. Biophys. Res. Commun. 56,* 807–814.
Shulman, R. G., Hopfield, J. J., and Ogawa, S. (1975), *Q. Rev. Biophys. 8,* 325–420.
Stein, A., and Crothers, D. M. (1976a), *Biochemistry 15,* 157–159.
Stein, A., and Crothers, D. M. (1976b), *Biochemistry 15,* 160–168.
Yang, S. K., and Crothers, D. M. (1972), *Biochemistry 11,* 4375–4381.

Changes in Tertiary Structure Accompanying a Single Base Change in Transfer RNA. Proton Magnetic Resonance and Aminoacylation Studies of *Escherichia coli* $tRNA^{Met}_{f_1}$ and $tRNA^{Met}_{f_3}$ and Their Spin-Labeled (s^4U8) Derivatives†

Walter E. Daniel, Jr.,‡ and Mildred Cohn*,§

ABSTRACT: The properties of *Escherichia coli* $tRNA^{Met}_{f_1}$ and $tRNA^{Met}_{f_3}$ that differ by only one base change, m^7G to A at position 47, have been compared structurally by proton magnetic resonance and functionally by the aminoacylation reaction. The NMR spectra of the two tRNA species in the region between 0 and 4 ppm below 4,4-dimethyl-4-silapentane-1-sulfonic acid (DSS) (methyl and methylene region) were the same except for the absence of the lowest field peak at 3.8 ppm in $tRNA^{Met}_{f_3}$, thus unequivocally identifying this resonance as the methyl group of m^7G47 of $tRNA^{Met}_{f_1}$. The same resonance disappears in $tRNA^{Met}_{f_1}$ spin-labeled at s^4U8 and reappears in the diamagnetic reduced spin-labeled $tRNA^{Met}_{f_1}$ from which the average distance between the spin-label and the methyl protons of m^7G is estimated to be less than 15 Å. The proximity of m^7G47 but not T55 to s^4U8 in the structure of *E. coli* $tRNA^{Met}_{f_1}$ in solution is consistent with the crystallographic model for yeast $tRNA^{Phe}$. A spectral comparison of the hydrogen-bond regions (11–14 ppm below DSS) of $tRNA^{Met}_{f_1}$ and $tRNA^{Met}_{f_3}$ reveals major shifts of four resonances previously assigned to tertiary hydrogen bonds. Of the four, the one at lowest field (14.8 ppm) had been assigned by chemical modification to the tertiary (s^4U8–A14) hydrogen bond and the one at 13.3 ppm had been tentatively assigned to the tertiary hydrogen bond G23–m^7G47 of the 13–23–47 triple. A more positive assignment of the G23–m^7G47 at 13.3 ppm could be made from the additional evidence that this resonance, which was first observed in the difference spectrum between spin-labeled $tRNA^{Met}_{f_1}$ and its reduced form, is the only one missing in the analogous difference spectrum of $tRNA^{Met}_{f_3}$. At low ionic strength and in the absence of magnesium ions, the differences in the hydrogen-bonded region of the NMR spectra of $tRNA^{Met}_{f_1}$ and $tRNA^{Met}_{f_3}$ are much greater than in the presence of magnesium ions. The optimal magnesium concentration required for maximal initial velocities is also higher for $tRNA^{Met}_{f_3}$ than for $tRNA^{Met}_{f_1}$. The perturbation caused by the spin-label in destabilizing hydrogen bonds in the region between 13 and 14 ppm is greater for $tRNA^{Met}_{f_3}$ than $tRNA^{Met}_{f_1}$ but the distance relations for the hydrogen bonds in the region between 12 and 13 ppm (the major paramagnetic perturbations) are conserved in the two species. The disruption of one hydrogen bond relative to native $tRNA^{Met}_{f_1}$ either by spin-labeling (s^4U8–A14) or by substitution of m^7G by A in $tRNA^{Met}_{f_3}$ has little effect on the aminoacyl acceptor activity or the velocity of the aminoacylation reaction at optimal magnesium concentration, but the absence of both tertiary hydrogen bonds in the augmented D-helix region in the spin-labeled $tRNA^{Met}_{f_3}$ results in approximately 60% reduction both in acceptance activity and in initial velocity of the aminoacylation reaction.

Since it is clear that the tertiary structure of tRNA is crucial for its recognition by the appropriate aminoacyl tRNA synthetase, we are attempting to establish quantitative indicators of tRNA tertiary structure in solution. Because the effect of a paramagnetic species on the relaxation time of a nuclear spin is a function of distance between the two, initially, the effects of a nitroxide spin-label covalently bound to s^4U at position 8 of *E. coli* $tRNA^{Met}_{f_1}$ on the ^1H NMR spectrum of the methyl region and of the ring NH hydrogen bond region were investigated (Daniel and Cohn, 1975). Without assigning the resonances to particular hydrogens, one can, of course, follow changes in conformation as reflected in changes in the spectra of the spin-labeled derivatives, but interpretation in terms of detailed structural change is possible only if each proton resonance is assigned.

In the earlier report, the lowest field methyl peak in the region of 0–4 ppm from DSS[1] was tentatively assigned to m^7G at position 47[2] based on the assignments in yeast $tRNA^{Phe}$ (Kan et al., 1974). A comparison of the proton resonances of

† From the Department of Biochemistry and Biophysics, University of Pennsylvania Medical School, Philadelphia, Pennsylvania, 19174. *Received February 6, 1976.* This work was supported by research grants from the United States Public Health Service (GM 12446) and from the National Science Foundation (GB32168). The 220 MHz spectra were taken at the Middle Atlantic NMR Research Facility supported by National Institutes of Health Grant RR-00542 and the 250 MHz spectra at the Mellon Institute NMR Facility for Biomedical Studies in Pittsburgh, Pennsylvania.

‡ Career Investigator Fellow of the American Heart Association.
§ Career Investigator of the American Heart Association.

[1] Abbreviations used are: DSS, 4,4-dimethyl-4-silapentane-1-sulfonic acid; DEAE, diethylaminoethyl; Hepes, *N*-2-hydroxyethylpiperazine-*N*′-3-propanesulfonic acid; EDTA, (ethylenedinitrilo)tetraacetic acid; ATP, adenosine 5′-triphosphate; SL, spin labeled; ESR, electron spin resonance; NMR, nuclear magnetic resonance.

$tRNA^{Met}_{f_3}$ that differs from $tRNA^{Met}_{f_1}$ only by substitution of A for m^7G leads to the unequivocal assignment of the methyl proton resonance of m^7G. Furthermore, in the earlier work a proper control was not available to separate the possible diamagnetic perturbation effects of the covalently bound spin-label from the paramagnetic effects on the protons in the methyl region of the spectrum. The difficulty arose because the proton resonances of the reductant, ascorbic acid (Kornberg and McConnell, 1971), usually used to produce the control, i.e., the diamagnetic reduced spin-labeled derivative, overlap the resonance peaks in the methyl region of tRNA. Another reductant for the nitroxide spin-label, phenylhydrazine (Rozantsev and Golubev, 1966), which does not suffer from this disadvantage has now been used to produce a suitable control for the methyl region of the spectrum of spin-labeled $tRNA^{Met}_{f_1}$. Consequently, interpretation is straightforward, since the paramagnetic contribution which is a direct function of the electron spin–nuclear spin distance can be separated from possible diamagnetic perturbations due to the spin-label modification.

In the hydrogen-bonded region of the spectrum of *E. coli* $tRNA^{Met}_{f_1}$ (11–15 ppm below DSS), four bonds of the 27 ± 1 total observed (Daniel and Cohn, 1975) are sufficiently close to the spin-label for the corresponding resonances to be severely broadened by the paramagnetic species. The resonances could be identified only tentatively based on earlier assignments of resonance positions from ring current theory (Shulman et al., 1973) and by analogy to the structure of yeast $tRNA^{Phe}$ derived from x-ray crystallographic data (Kim et al., 1974; Robertus et al., 1974b). Similarity of chemical reactivity, i.e., base accessibility of yeast $tRNA^{Phe}$ and *E. coli* $tRNA^{Met}_{f_1}$, both class I tRNA's, has been cited as support for similarity of tertiary structures (Clark, 1975). A plausible assignment for the paramagnetically broadened peak at lowest field, 13.3 ppm, designated f (Daniel and Cohn, 1975) was the G23-m^7G47 hydrogen bond of the 13–23–47 triple based on proximity arguments using the crystallographic model of the $tRNA^{Phe}$ structure with its corresponding 13–22–46 triple (Kim et al., 1974) (see Figure 1C). It was suggested that a definitive answer could come from the spectrum of *E. coli* $tRNA^{Met}_{f_3}$ that lacks a 23–47 bond of the type shown in Figure 1C, since position 47 is now occupied by A rather than m^7G. In this report, the low field spectra of $tRNA^{Met}_{f_1}$ and $tRNA^{Met}_{f_3}$ are compared for purposes of peak assignment and of determining the effect on the tertiary structure of the loss of a single tertiary hydrogen bond between the dihydro-U stem and the extra loop. Differences in structural stability of the two fMet-tRNA's in the region of the dihydro-U helix and "tertiary interactions" had been noted by Crothers et al. (1974), since they observed a melting transition for f_1Met at 46 °C (ΔH = 52 kcal/mol) and a different one for f_3Met at 30 °C (ΔH = 30 kcal/mol). In addition, structural differences in the s^4U8 region of the molecule had been inferred from differences in the respective abilities of the two tRNA's to form the photochemically induced cross-linked product between s^4U8 and C13 (Delaney et al., 1974). It had been noted from the x-ray crystallographic data on yeast $tRNA^{Phe}$ (Kim et al., 1974) that the positively charged m^7G is involved in an ionic interaction with nearby phosphate groups; this type of interaction is precluded upon substitution of m^7G by A.

Experimental Procedure

Materials

Benzoylated DEAE-cellulose and DEAE-Sephadex A-50 were products of Schwarz/Mann and Pharmacia Fine Chemicals, Inc., respectively. The resin, RPC-5 was the gift of D. Novelli of Oak Ridge National Laboratory. Transfer $RNA^{Met}_{f_3}$ from *E. coli* K-12 (Oak Ridge lot no. 18-123) in partially purified form was a gift from J. Ofengand of the Roche Institute of Molecular Biology and A. D. Kelmers of Oak Ridge National Laboratory. The *E. coli* methionyl-tRNA synthetase was a generous gift from J. P. Waller of the Ecole Polytechnique.

Radioactive methionine ^3H or ^{14}C was purchased from Schwarz/Mann, and deuterium oxide (99.9%) from Thompson Packard. All other chemicals used were reagent grade. The membrane filters (RAWP) were purchased from the Millipore Corp.

Methods

Preparation of $tRNA^{Met}_{f_1}$. Highly purified $tRNA^{Met}_{f_1}$ was prepared from unfractionated *E. coli* B tRNA (Schwarz/Mann lot no. Y2106) by three chromatographic steps: (i) benzoylated DEAE-cellulose column chromatography at 5 °C, with pH 5.0 buffers, containing magnesium (Roy et al., 1971), (ii) chromatography of the combined enriched $tRNA^{Met}$ fractions on DEAE-Sephadex A-50 columns at pH 7.5, 25 °C, with an eluting buffer containing 375 mM sodium chloride (Seno et al., 1968), and (iii) benzoylated DEAE-cellulose column chromatography at pH 6.0 and 5 °C to resolve $tRNA^{Met}_{f_1}$ from $tRNA^{Met}_{m}$. During the preparative steps, light was excluded to prevent photochemical cross-linking of s^4U8 to C13 (Favre et al., 1971). Chromatography on RPC-5 (Egan et al., 1973) of the resulting $tRNA^{Met}_{f_1}$ indicated no detectable amount of photocross-linked derivative and less than 5% contamination with other tRNA's.

Preparation of E. coli $tRNA^{Met}_{f_3}$. The $tRNA^{Met}_{f_3}$ from Oak Ridge National Laboratory (~1000 A_{260} units; lot no. 18-123) was purified by a single chromatographic step on RPC-5 (1.0 × 115 cm column) at 37 °C. A linear gradient of 3000 ml from 0.05 M Tris-HCl, pH 7.0, 0.01 M $MgCl_2$, and 0.45 M NaCl to 0.05 M Tris-HCl, pH 7.0, 0.01 M $MgCl_2$, and 0.65 M NaCl were used.[3] The fractions of the large methionine-accepting peak were pooled, desalted, and utilized for the $tRNA^{Met}_{f_3}$ experiments.

Preparation of Spin-Labeled and Reduced Spin-Labeled Methionine tRNA's. The preparation of the nitroxide spin-label, *N*-(2,2,5,5-tetramethyl-3-pyrrolidinyl-1-oxy)bromoacetamide, has been described previously (Daniel et al., 1973). The extent of spin-labeling of s^4U8 of either $tRNA^{Met}_{f_1}$ or $tRNA^{Met}_{f_3}$ was followed by the decrease in absorbance at 335 nm (Hara et al., 1970). In either case, double integration of the nitroxide ESR signal of the spin-labeled tRNA yielded 1 ± 0.05 mol of unpaired electron spins per mol of tRNA.

For the NMR experiments in which the hydrogen-bonded protons were being observed in the low-field region (11–15 ppm from DSS), the nitroxide of either SL-s^4U-$tRNA^{Met}_{f}$ could be reduced to the diamagnetic hydroxylamine with ascorbate (Kornberg and McConnell, 1971). Five microliters of freshly prepared sodium ascorbate, 765 mM, pH 7, was added to 250 μl of 1.5 mM SL-s^4U-$tRNA^{Met}_{f}$ and the reduction proceeded

[2] *E. coli* $tRNA^{Met}_{f}$ has nine bases (14–22) in the dihydro-U loop compared to eight bases in yeast $tRNA^{Phe}$ (14–21); consequently, any base numbered *n* beyond residue 22 of *E. coli* $tRNA^{Met}_{f}$ will correspond to base numbered $n - 1$ in yeast $tRNA^{Phe}$, e.g., m^7G47 of *E. coli* $tRNA^{Met}_{f}$ corresponds to m^7G46 in yeast $tRNA^{Phe}$.

[3] Procedure suggested by A. D. Kelmers (personal communication).

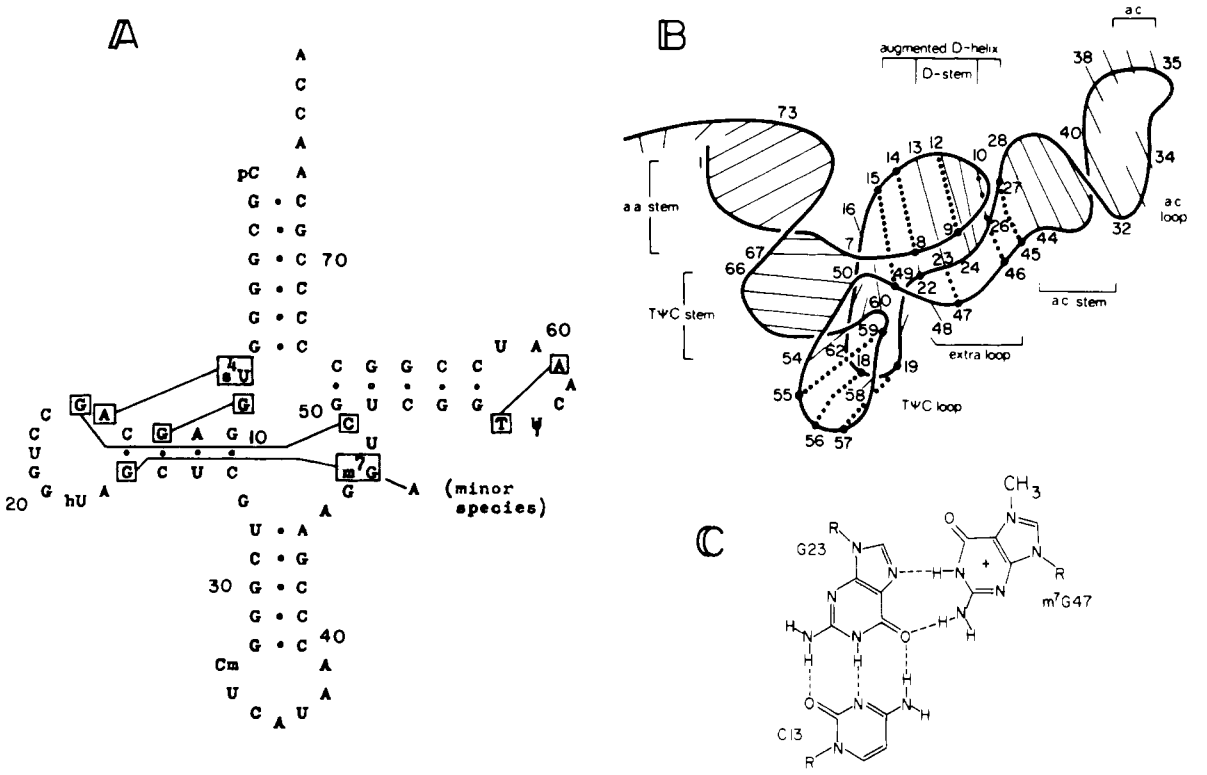

FIGURE 1: (A) The cloverleaf structure of *E. coli* $tRNA^{Met}_{f_1}$ with indicated change at position 47 for $tRNA^{Met}_{f_3}$; the solid lines indicate some of the probable tertiary hydrogen bonds for $tRNA^{Met}_{f_1}$. (B) Schematic representation of the proposed tertiary structure of *E. coli* $tRNA^{Met}_{f_1}$ based on the representation of the crystallographic model of yeast $tRNA^{Phe}$ (Ladner et al., 1975). All residue numbers beyond residue 21 in *E. coli* $tRNA^{Met}_f$ are greater by 1 than the corresponding residues in the yeast $tRNA^{Phe}$ structure, since the D loop has one more residue in $tRNA^{Met}_f$ than in $tRNA^{Phe}$. The triple G9–G12–C24 with two tertiary hydrogen bonds between G9 and G12 indicated has been postulated (Kim et al., 1974) as a substitute for A9–A23–U12 triple of yeast $tRNA^{Phe}$ with two tertiary bonds between A9 and A23. (C) The detailed structure of the C13–G23–m^7G47 triple possible in $tRNA^{Met}_{f_1}$; in the $tRNA^{Met}_{f_3}$ species with A replacing m^7G at 47, effective pairing with G23 is not possible and any pairing would yield no NMR signal in the range of 11–15 ppm from DSS.

for 4 h in the NMR tube under a nitrogen atmosphere before NMR spectra were recorded. Analysis of the samples by ESR indicated greater than 99% of the nitroxide was reduced by this procedure. The original ESR signal was fully recoverable on exposure of the sample to oxygen for several hours.

In an experiment in which the odd base methyl and methylene resonances were to be observed in D_2O, phenylhydrazine (Rozantsev and Golubev, 1966) was chosen to reduce the nitroxide moiety of SL-s^4U-$tRNA^{Met}_{f_1}$, since ascorbate gives proton resonances at high field (0–4 ppm from DSS). Five microliters of a phenylhydrazine solution, 765 mM, pH 7.0, was added to 250 μl of SL-s^4U-$tRNA^{Met}_{f_1}$ (1.5 mM) in a sodium phosphate buffer, pH 7.0, containing 100 mM NaCl and 5 mM $MgCl_2$. The reduction proceeded for 5 h at room temperature under nitrogen before the spectrum in Figure 2C was obtained. The remaining ESR signal intensity of the sample indicated the reduction was ~85% complete.

Aminoacylation of tRNA. The assay mixtures (50 or 100 μl) contained 20 mM Hepes, pH 7.5, 2 mM ATP, 10 μM EDTA, 30 mM 2-mercaptoethanol. For methionine acceptance determinations, the solutions contained 150 mM NH_4Cl and 10 mM $MgCl_2$. For initial rate experiments, the reaction was initiated by addition of synthetase after equilibration at 25 °C. The reaction was stopped at appropriate time intervals by addition of 2 ml ice-cold 5% trichloroacetic acid. After 10 min at 0 °C, the precipitate was collected on a Millipore filter. The reaction tube was rinsed three times with 5% trichloroacetic acid, and the washings were poured through the filter. The filter was washed once more and, after removal of the upper part of the filter holder, the filter was washed several times with cold 5% Cl_3CCOOH and then sucked dry. The extensive washing procedure lowered the background radioactivity to approximately 0.01% of the total counts in the reaction mixture. The Millipore filter was dissolved in 5 ml of Bray's solution and the radioactivity (^{14}C or ^3H) was measured in a Beckmann Scintillation counter LS-100C.

NMR and ESR Measurements. Solutions of tRNA or of spin-labeled derivatives ~50 mg/ml were prepared for NMR measurements by extensive dialysis in a microcell at 5 °C against the appropriate H_2O or D_2O buffer. Prior to being transferred to the NMR tube, the dialyzed solutions were centrifuged to remove any insoluble material. The sample volumes for NMR were between 200 and 250 μl and ~50 μl for ESR.

Spectra of the odd base methyl region (0–4 ppm from DSS) were obtained in D_2O solution by Fourier transform spectroscopy with a Varian HR220 MHz NMR spectrometer. Spectra of the slowly exchanging hydrogen-bonded protons at low field (11–15 ppm from DSS) were recorded in H_2O solution either with a 250 MHz spectrometer with correlation spectroscopy or with a 220 MHz spectrometer with signal averaging. ESR spectra of the spin-labeled tRNA were recorded on a Varian E-4 ESR spectrometer. A Nicolet Model 1074 computer interfaced with the ESR spectrometer permitted spin quantitation.

Results

Proton NMR of Methyl and Methylene Groups. From the base composition shown in Figure 1A, there are four groups of protons in *E. coli* $tRNA^{Met}_{f_1}$ with resonance peaks in the

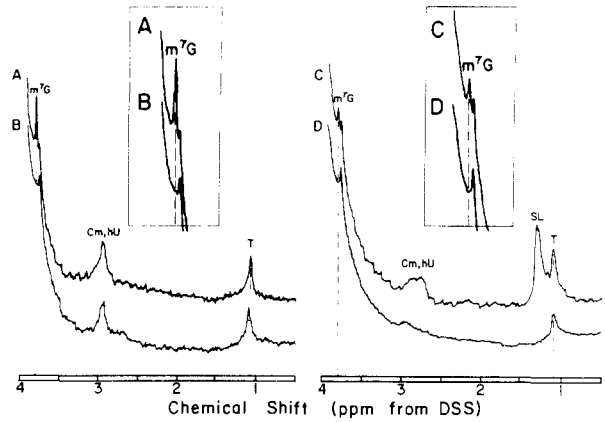

FIGURE 2: 220 MHz FT ^{1}H NMR spectra of odd base methyl and methylene groups in the high-field region, 0–4 ppm from the internal standard DSS. (A) Native $tRNA^{Met}_{f_1}$, (B) native $tRNA^{Met}_{f_1}$, (C) phenylhydrazine-reduced SL-s^4U-$tRNA^{Met}_{f_1}$, (D) SL-s^4U-$tRNA^{Met}_{f_1}$. Samples A, B, and D had been dialyzed against 20 mM sodium phosphate, pH 7.0, 100 mM NaCl, and 5 mM $MgCl_2$ in D_2O. Sample C was prepared by adding phenylhydrazine in the same phosphate buffer, pH 7.0, directly to sample D under a nitrogen atmosphere. Spectra were accumulated for 2–3 h at 37 °C; 3600 transients (with block averaging: 150 transients/block).

high-field region between DSS and 4 ppm below it, the methyl resonances of (1) 2′-*O*-methylcytidine-33 (C_M), (2) 7-methylguanosine-47 (m^7G), (3) ribothymidine-55 (T), and the methylene resonances of (4) dihydrouridine-21 (C5-hU and C6-hU); in $tRNA^{Met}_{f_3}$, one methyl group arising from m^7G is lacking. The earlier assignments for $tRNA^{Met}_{f_1}$ (Daniel and Cohn, 1975) based on the yeast $tRNA^{Phe}$ assignments (Kan et al., 1974) are indicated in Figure 2A. A comparison of the high-field resonances of *E. coli* $tRNA^{Met}_{f_1}$ and $tRNA^{Met}_{f_3}$ (curves A and B, respectively, and inserts of Figure 2) clearly shows that they differ only in the absence of the resonance at lowest field, 3.80 ppm, in $tRNA^{Met}_{f_3}$, thus unequivocally confirming the earlier assignment of this peak to m^7G at position 47.

The disappearance of the m^7G resonance peak in the spin-labeled derivative of $tRNA^{Met}_{f_1}$, curve D of Figure 2, might be ascribed to a paramagnetic broadening due to the spin-label, i.e., proximity of m^7G47 to s^4U8 (cf. Figure 1B). Alternatively, a structural perturbation introduced by the spin-label modification could result in a downfield diamagnetic shift of the resonance at 3.80 ppm completely obscuring the methyl resonance of m^7G under the large peak below 4 ppm. The partial reappearance of the peak at 3.80 ppm upon partial reduction (~85%) of the nitroxide free radical with phenylhydrazine (curve C of Figure 2) eliminates the possibility of ascribing the spin-label effect on this resonance peak to a structural perturbation, and establishes the proximity of m^7G at position 47 to s^4U8 for the $tRNA^{Met}_{f_1}$ structure in solution. It should be noted in curve C that the reduction of the spin-label may be monitored not only by the disappearance of the ESR signal but also by the appearance of the methyl groups of the spin-label itself as seen at 1.3 ppm in curve C of Figure 2.

Low-Field N–H Bonds. In Figure 3, the spectra of *E. coli* $tRNA^{Met}_{f_1}$ (top curve) and $tRNA^{Met}_{f_3}$ (middle curve) in H_2O solutions containing 100 mM NaCl, 5 mM $MgCl_2$, and 20 mM sodium phosphate buffer, pH 7.0, are compared in the region between 11 and 15 ppm below DSS. Although only one base m^7G47 and consequently one tertiary bond must disappear, in fact, four resonance peaks are clearly affected, as shown in the difference spectrum at the bottom of Figure 3. Since the

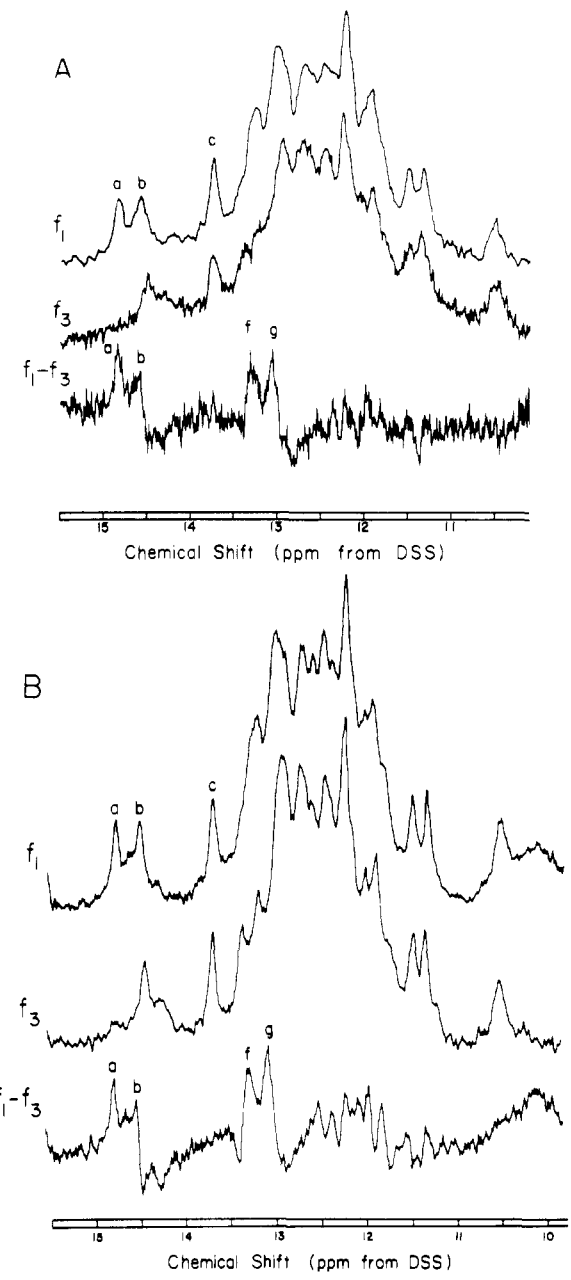

FIGURE 3: Hydrogen bond CW-NMR spectra (A) at 220 MHz and (B) 250 MHz in the region 11–15 ppm downfield from DSS. *Top spectrum*, native $tRNA^{Met}_{f_1}$; *middle spectrum*, $tRNA^{Met}_{f_3}$; *bottom spectrum*, the difference spectrum $tRNA^{Met}_{f_1}$ minus $tRNA^{Met}_{f_3}$. Each sample was prepared by extensive dialysis against 20 mM sodium phosphate, pH 7.0, 100 mM NaCl, and 5 mM $MgCl_2$ in H_2O. Spectra represent 2400 scans at 30 °C.

difference spectrum at 220 MHz was rather noisy, the spectra were recorded again at 250 MHz using correlation spectroscopy as shown in Figure 3B. Again, the most significant differences between $tRNA^{Met}_{f_1}$ and $tRNA^{Met}_{f_3}$ fall at the resonances labeled a, b, f, g (Daniel and Cohn, 1975). The perturbed peaks were previously assigned to tertiary hydrogen bonds, (cf. Figure 1B); peak a was unambiguously assigned to s^4U8–A14, peaks b, f, and g were tentatively assigned to G9–G12, G23–m^7G47, and G15–C49, respectively (Daniel and Cohn, 1975). In the absence of magnesium ions and at lower ionic strength, i.e., in solutions containing 30 mM NaCl, 10 mM sodium phosphate, pH 7.0, and 0.1 mM EDTA, the differences in structure of the two tRNA's are even greater, as evidenced by the low field spectra shown in Figure 4. Not

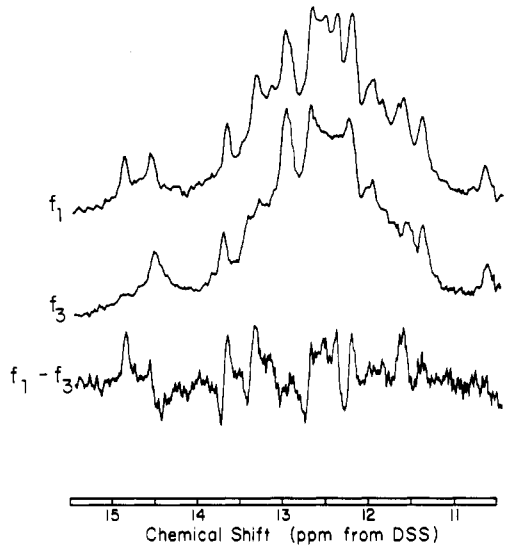

FIGURE 4: Hydrogen bond CW-NMR spectra at 220 MHz in the region, 11-15 ppm downfield from DSS. *Top spectrum,* $tRNA^{Met}_{f_1}$; *middle spectrum,* $tRNA^{Met}_{f_3}$; *bottom spectrum,* the difference spectrum $tRNA^{Met}_{f_1}$ minus $tRNA^{Met}_{f_3}$. The samples were prepared by dialysis first against 10 mM sodium phosphate, pH 7.0, 300 mM NaCl, and 0.1 mM EDTA in H_2O, and then extensively against 10 mM sodium phosphate, pH 7.0, 30 mM NaCl, and 0.1 mM EDTA in H_2O. Approximately 3000 scans were averaged at 30 °C.

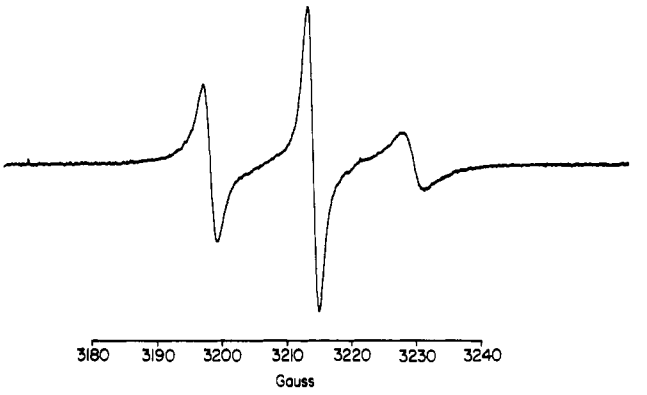

FIGURE 5: EPR spectrum observed for either SL-s^4U-$tRNA^{Met}_{f_1}$ or SL-s^4U-$tRNA^{Met}_{f_3}$, approximately 1.5 mg/ml in 20 mM sodium phosphate, pH 7.0, 100 mM NaCl, and 5 mM $MgCl_2$ in H_2O. The spectrum was recorded at 26 °C and a modulation amplitude of 1 G.

only are the regions of the molecule represented by the N-H bonds corresponding to a, b, and f structurally different in $tRNA^{Met}_{f_3}$ and $tRNA^{Met}_{f_1}$ but at low salt in the absence of Mg^{2+}, many other hydrogen bonds are shifted as well.

Spin-Labeled tRNA. Since both peaks f and g appear in the difference spectrum of Figure 3A, it is difficult to decide whether the two shifted or which, if any, disappeared. Consequently, an unambiguous choice could not be made between peak f or g in assigning the resonance peak of the G23-m^7G47 tertiary bond. This difficulty was obviated by comparing the spin-labeled derivatives of $tRNA^{Met}_{f_1}$ and $tRNA^{Met}_{f_3}$ with their reduced forms. The rationale is that in $tRNA^{Met}_{f_3}$ there should be no difference spectrum in the peak position corresponding to the nonexistent G23-m^7G47 tertiary hydrogen bond, but such a hydrogen if close to s^4U8 would show up in the difference spectrum between the spin-labeled and reduced spin-labeled $tRNA^{Met}_{f_1}$.

Both tRNA species were spin-labeled and the ESR spectra shown in Figure 5 were identical for both species. Whatever structural differences exist are obviously not reflected in the ESR spectra and, consequently, do not affect the mobility of the spin-label. A comparison of the low-field ^{1}H NMR spectra of the spin-labeled and of the reduced spin-labeled forms and of the differences between them is presented for $tRNA^{Met}_{f_1}$ and $tRNA^{Met}_{f_3}$ in Figure 6. Peaks g, h, and i are essentially the same in the difference spectrum of $tRNA^{Met}_{f_1}$ (curve C_1 of Figure 6) and of $tRNA^{Met}_{f_3}$ (curve C_3 of Figure 6). Therefore, peak f rather than peak g may be assigned to the tertiary bond G23-m^7G47.

The small residual peak at position f in the difference spectrum of spin-labeled and reduced spin-labeled $tRNA^{Met}_{f_3}$ (curve C_3, Figure 6), if not within experimental error, may well be due to the fact that peak f at 13.3 ppm is a composite paramagnetically broadened peak with contributions not only from the tertiary G23-m^7G47 bond but also the secondary G50-C66 bond that also falls in this region of the spectrum (Shulman et al., 1973). An examination of the three-dimensional model of yeast $tRNA^{Phe}$ in the laboratory of A. Rich showed that a spin-label at position 8 could come close to the hydrogen bond m^5C49-G65 (G50-C66 in $tRNA^{Met}_f$) as well as to the tertiary hydrogen bond G22-m^7G46 (G23-m^7G47 in $tRNA^{Met}_{f_1}$). Alternatively, the residual peak at 13.3 ppm may be ascribed to the G12-C24 Watson-Crick pair in $tRNA^{Met}_{f_3}$ (see assignments, Figure 6). The latter assignment, which implies that the G9-G12-C24 triple is closer to s^4U8 in $tRNA^{Met}_{f_3}$ than in $tRNA^{Met}_{f_1}$, would also account for a small peak b′ (14.1 ppm) assigned to G9-G12 tertiary bond of the G9-G12-C24 triple (cf. curves C_1 and C_3). Our assignment of peak g at 12.9 ppm to G15-C49 remains tentative, based on proximity arguments in the spin-labeled $tRNA^{Met}_f$; this band appears to be perturbed in $tRNA^{Met}_{f_3}$ as are the other tertiary bonds in this part of the molecule. Although an N-H-O bond might be expected to fall at higher field as pointed out by Reid and Robillard (1975) and as observed for a model compound at 11.9 ppm by Kallenbach et al., (1976), the assignment of a hydrogen bond to a reverse Watson-Crick base pair at 12.9 ppm is not unreasonable if it were not subject to upfield shifts from strong ring current effects.

Comparison of Kinetic Properties of $tRNA^{Met}_{f_1}$ and $tRNA^{Met}_{f_3}$ in the Aminoacylation Reaction

Methionine Acceptance Activity, K_M and V_{Max}. The methionine acceptance activities (pmol/A_{260} unit) were found to be: $tRNA^{Met}_{f_1}$, 1400; SL-$tRNA^{Met}_{f_1}$, 1400; $tRNA^{Met}_{f_3}$, 1100; SL-$tRNA^{Met}_{f_3}$, 430. The dependence of kinetic parameters of the reaction for $tRNA^{Met}_{f_1}$ has been thoroughly investigated by Lawrence et al. (1973). Although a different buffer has been used in the experiments listed in Table I, the values of K_M and V_{Max} for $tRNA^{Met}_{f_1}$ in the presence of Mg^{2+} agree well with those previously reported. The observation that NH_4^+ alone stimulated the reaction under conditions where KCl does not, confirms the findings of Lawrence et al., (1973). As shown in Table I, the K_M values for $tRNA^{Met}_{f_3}$ under all conditions are somewhat larger than for $tRNA^{Met}_{f_1}$. The values of V_{Max}, on the other hand, are about the same for $tRNA^{Met}_{f_1}$ and $tRNA^{Met}_{f_3}$ in the presence of Mg^{2+} but much lower for $tRNA^{Met}_{f_3}$ in the presence of NH_4^+ alone. The concentrations of Mg^{2+} used in these experiments, 4 mM for $tRNA^{Met}_{f_1}$ and 5 mM for $tRNA^{Met}_{f_3}$, are those that yielded maximal initial velocities in the aminoacylation reaction (cf. Figure 7).

Effect of Mg^{2+} Concentration on Initial Rates. Since structural differences between $tRNA^{Met}_{f_1}$ and $tRNA^{Met}_{f_3}$ as monitored by the chemical shifts of the hydrogen bond resonances shown above and by the rates of the photochemical

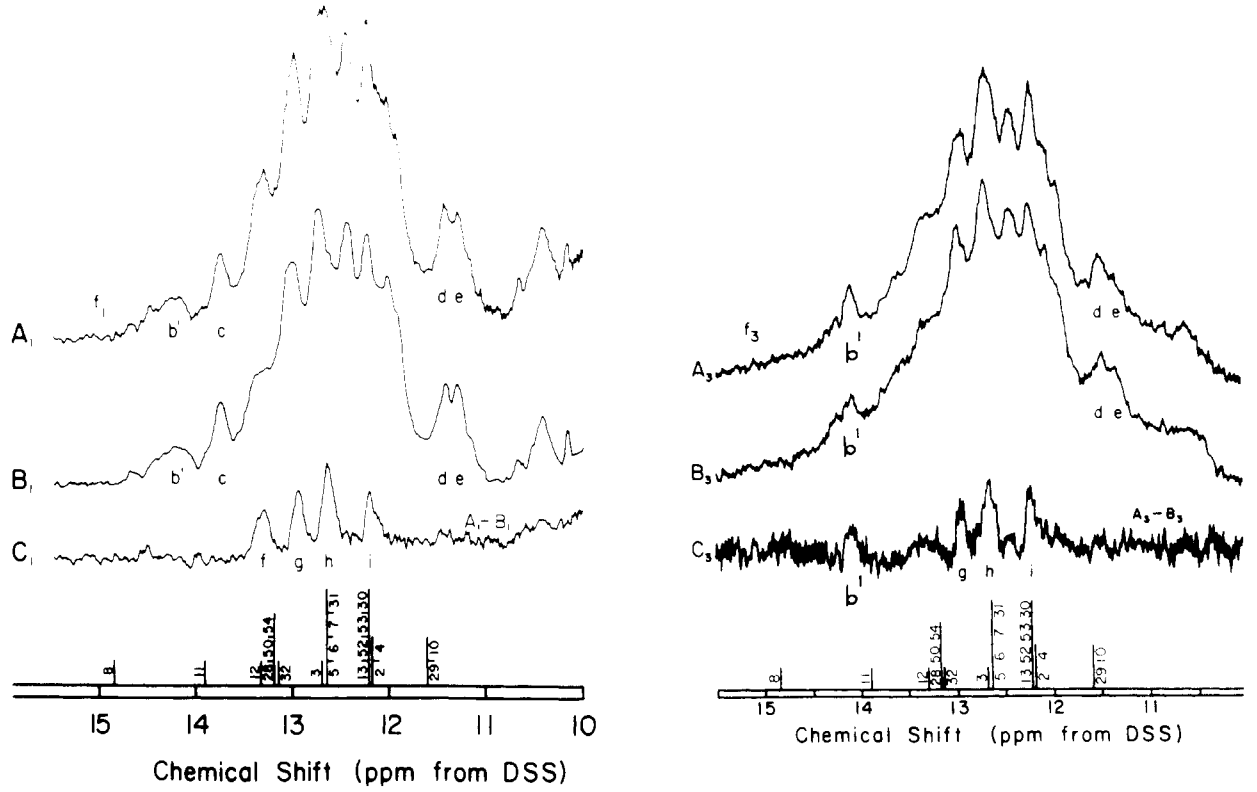

FIGURE 6: Proton NMR spectra of the hydrogen-bonded ring nitrogen protons of tRNA derivatives in the region, 11-15 ppm from DSS. Series A, 250 MHz spectra: (A_1) ascorbate-reduced SL-s^{4}U-tRNA$^{Met}_{f_1}$; (B_1) SL-s^{4}U-tRNA$^{Met}_{f_1}$; (C_1) difference spectrum, A_1 minus B_1. Series B, 220 MHz spectra: (A_3) ascorbate-reduced SL-s^{4}U-tRNA$^{Met}_{f_3}$; (B_3) SL-s^{4}U-tRNA$^{Met}_{f_3}$; (C_3) difference spectrum, A_3 minus B_3. All samples had been dialyzed against 20 mM sodium phosphate, pH 7.0, 100 mM NaCl, and 5 mM $MgCl_2$. In series A, 600–2000 scans were accumulated at 30 °C with correlation spectroscopy using a sweep width of 1500 Hz and sweep time 5 s. In series B, approximately 2500 scans were averaged for each spectrum at 30 °C. The calculated positions (Shulman et al., 1973) of the secondary structure hydrogen bonds are shown. The s^{4}U8 tertiary hydrogen bond assignment is based on chemical modification (Daniel and Cohn, 1975).

TABLE I: Comparison of K_M and V_{Max} of *E. coli* tRNA$^{Met}_{f_1}$ and tRNA$^{Met}_{f_3}$ for *E. coli* Methionine tRNA Synthetase at 25 °C.[a]

	tRNA$^{Met}_{f_1}$			tRNA$^{Met}_{f_3}$	
Salts Added	K_M (μM)	V_{Max}	Salts Added	K_M (μM)	V_{Max}
100 mM NH_4Cl	1.0	0.106	100 mM NH_4Cl	1.9	0.026
200 mM NH_4Cl	1.55	0.79	200 mM NH_4Cl	3.3	0.18
4 mM $MgCl_2$	0.75	8.3	5 mM $MgCl_2$	1.0	11.1
4 mM $MgCl_2$ + 150 mM NH_4Cl	1.3	33.3	5 mM $MgCl_2$ + 150 mM NH_4Cl	5.0	33.3

[a] The solutions contained 20 mM sodium Hepes, pH 7.5, 2 mM ATP, 32 μM methionine (^{3}H, 1.2 × 10^7 cpm/ml), and salt concentration as indicated. V_{Max} in all experiments is expressed as pmol of Met-tRNA formed min^{-1} ml^{-1} with 80 pmol of pure methionine synthetase, the enzyme concentration actually used in experiments with $MgCl_2$; in the absence of $MgCl_2$, the concentration of active enzyme was increased 15-fold and crude synthetase was used.

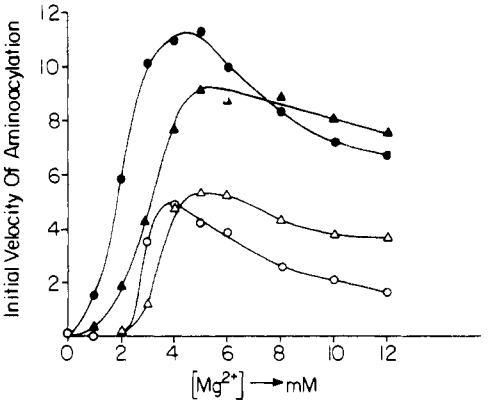

FIGURE 7: A comparison of the rate of aminoacylation of tRNA$^{Met}_{f_1}$ and tRNA$^{Met}_{f_3}$ as a function of $MgCl_2$ concentration. The solutions contained in a total volume of 50 μl: 20 mM potassium Hepes, pH 7.5, 2 mM ATP, 30 μM EDTA, 10 μg bovine serum albumin/ml, 25 mM β-mercaptoethanol; in the two upper curves 150 mM NH_4Cl was also present; T = 25 °C. The rates were linear over the 10-min period before termination. (O—O, ●—●) tRNA$^{Met}_{f_1}$, (△—△, ▲--▲) tRNA$^{Met}_{f_3}$.

cross-linking reaction (Delaney et al., 1974) were dependent on the Mg^{2+} concentration, an attempt was made to correlate these differences with the rates of aminoacylation catalyzed by *E. coli* methionine-tRNA synthetase as a function of Mg^{2+} concentration. The kinetic experiments were carried out under conditions similar to those used by Lawrence et al., (1973) and the results are plotted in Figure 7 in the form of initial rate vs. $MgCl_2$ concentration with and without 150 mM NH_4Cl. The results for tRNA$^{Met}_{f_1}$ are very similar to those found by the earlier investigators (Lawrence et al., 1973). For tRNA$^{Met}_{f_3}$ more Mg^{2+} is required to yield the same optimal rates as found for tRNA$^{Met}_{f_1}$ in the presence or absence of 150 mM NH_4Cl. However, at concentrations of Mg^{2+} beyond the optimal one, the rate falls off more rapidly for tRNA$^{Met}_{f_1}$ and, consequently, is slightly higher for tRNA$^{Met}_{f_3}$ than for tRNA$^{Met}_{f_1}$ in this range. Since SL-tRNA$^{Met}_{f_3}$ had a methionine acceptance value only 39% of the native form, its rate of aminoacylation was

TABLE II: Calculations of r for Various Values of $\tau_c/(\Delta\upsilon)_p$.

$\tau_c/(\Delta\upsilon)_p$	r^a (Å)
10^{-12}	5.3
10^{-11}	7.7
10^{-10}	11.3
10^{-9}	16.6
10^{-8}	24.4
10^{-7}	35.8

[a] The distance, r, between the electron spin of the nitroxide radical and a proton as a function of $\tau_c/(\Delta\upsilon)_p$, where τ_c is the correlation time modulating the interaction between the electron spin and the proton spin and $(\Delta\upsilon)_p$ is the paramagnetic contribution to the line width of the proton. The values of r were calculated from the Solomon-Bloembergen equation with three assumptions: (1) no hyperfine interaction, (2) $\tau_c = T_{2e}$, (3) $\omega_s^2\tau_c^2 \gg 1$.

compared to those of native tRNA$^{Met}_{f_1}$ and tRNA$^{Met}_{f_3}$. The relative initial velocities in the presence of 5.5 mM $MgCl_2$ were found to be tRNA$^{Met}_{f_3}$ 100, SL-tRNA$^{Met}_{f_3}$ 42.5, tRNA$^{Met}_{f_1}$ 75.5; the concentrations of tRNA in this experiment were 3, 4, and 2.7 μM, respectively.

Discussion

In a comparison of tRNA$^{Met}_{f_1}$ and tRNA$^{Met}_{f_3}$ the predictable differences in the NMR spectra, namely, the absence in tRNA$^{Met}_{f_3}$ of the methyl resonance due to m^7G47 and of the tertiary hydrogen bond resonance due to G23-m^7G47, can be used to make assignments. On the other hand, the unpredictable differences, if any, may be used to delineate changes in structure that result from the loss of the tertiary bond G23-m^7G47. Thus, the tentative assignment of the methyl resonance at ~3.80 ppm to m^7G47 (Daniel and Cohn, 1975) has now been established unequivocally. Furthermore, it has also been established by a comparison of the methyl group spectra of partially r*educed* SL-tRNA$^{Met}_{f_1}$ with SL-tRNA$^{Met}_{f_3}$ that the methyl group of m^7G47 is close enough to the spin-label at s^4U8 in tRNA$^{Met}_{f_1}$ to be broadened sufficiently to become unobservable. The distance, r, required to effect such a broadening depends on τ_c and is given by the equation:

$$r \text{ (in Å)} = 525\,[\tau_c/(\Delta\upsilon)_p]^{1/6}$$

where the symbols are: τ_c, the correlation time ($1/\tau_c = 1/\tau_r + 1/\tau_e$) in seconds; $(\Delta\upsilon)_p$, paramagnetic contribution to the line width in Hz; τ_r, rotational correlation time, and τ_e, electron spin relaxation time. Calculations based on the equation above are listed in Table II. If we assume that in this particular case where only the top of the peak is visible (see Figure 2A), a broadening of ~20 Hz might well make it disappear and that from the ESR line shape, Figure 5, the correlation time is of the order of $1\text{-}5 \times 10^{-9}$ s, then the average distance between the methyl protons of m^7G47 and the spin-label is less than ~15 Å. This value is not inconsistent with the distance between U8 and m^7G46 in the crystallographic model for yeast tRNA^{Phe} (see Figure 1C). Thus, insofar as the proximity of residue 8 and the extra loop residue 47 (46 in Phe) is used as a criterion, the structure of *E. coli* tRNA$^{Met}_{f_1}$ in solution is similar to crystalline yeast tRNA^{Phe}.

An assignment of the tertiary bond between G23 and m^7G47 (Figure 1C) to the resonance f at ~13.3 ppm was made from the combined data of (1) the difference spectrum between native tRNA$^{Met}_{f_1}$ and tRNA$^{Met}_{f_3}$ (Figure 3) and (2) the difference spectra of SL-tRNA and reduced SL-tRNA of tRNA$^{Met}_{f_1}$ and tRNA$^{Met}_{f_3}$, respectively (Figure 6). The first difference spectrum is consistent with such an assignment and the second set of difference spectra strongly supports it.

It is not surprising that the absence of hydrogen bonds between the dihydro-U stem (G23) and the extra loop or at best, the retention of only a single hydrogen bond between A47N6 to G23, would induce structural changes in tRNA$^{Met}_{f_3}$ relative to tRNA$^{Met}_{f_1}$, although the nature of the changes is not predictable. In fact, a comparison of Figures 3 and 4 shows that the difference spectrum of the hydrogen-bond resonances between tRNA$^{Met}_{f_1}$ and tRNA$^{Met}_{f_3}$ depends on the ionic environment; at low salt concentration in the absence of Mg^{2+}, a considerably greater number of bonds are perturbed both in chemical shift and line width. Although the additional changes occurring at low salt concentration cannot at present be assigned to specific bonds, the finding is consistent with earlier work on photochemical cross-linking between s^4U8 and C13 (Delaney et al., 1974) that indicated that in 40 mM Na^+ cross-linking was virtually abolished in tRNA$^{Met}_{f_3}$, but in the presence of Mg^{2+}, the rate for tRNA$^{Met}_{f_3}$ was lowered only twofold relative to tRNA$^{Met}_{f_1}$. Major spectral differences between tRNA$^{Met}_{f_1}$ and tRNA$^{Met}_{f_3}$ in the N-H region of solutions containing high salt in the presence of Mg^{2+} are restricted to four bonds, all of which have been assigned to tertiary hydrogen bonds (a, 8-14; b, 9-12; g, 15-49; f, 23-47 (Figure 1B)) in the most congested region of the molecule involving the augmented D helix, the D stem, the extra loop, and the majority of the tertiary interactions. This finding is consistent with the earlier observation of Crothers et al. (1974) that the difference in stability between tRNA$^{Met}_{f_1}$ and tRNA$^{Met}_{f_3}$ is observed only for one melting transition involving the dihydro-U helix.

It will be noted that of the observable chemical shift changes in the NH region, between tRNA$^{Met}_{f_1}$ and tRNA$^{Met}_{f_3}$, only resonances assigned to tertiary bonds have been shifted and all have been shifted upfield in tRNA$^{Met}_{f_3}$. At this time, it is premature to interpret the upfield shifts in structural terms. If, and when models of the three-dimensional structures of *E. coli* tRNA$^{Met}_{f_1}$ and tRNA$^{Met}_{f_3}$ are available from crystallographic studies, then the direction and magnitude of the observed chemical shift differences of the hydrogen bonds, as well as the change between tRNA$^{Met}_{f_1}$ and tRNA$^{Met}_{f_3}$ in distance of the 9-12-24 triple to s^4U8, should be consistent with the postulated models. Since the same peaks, g,[4] h, and i are paramagnetically broadened by the spin-label at s^4U8, the geometry of those hydrogen bonds relative to s^4U8 should be conserved for tRNA$^{Met}_{f_1}$ and tRNA$^{Met}_{f_3}$ in the crystalline state as well.

The question of interest is how important are the structural alterations between tRNA$^{Met}_{f_1}$ and tRNA$^{Met}_{f_3}$ to their respective functions as methionyl acceptors. The loss of the s^4U8-A14 hydrogen bond by spin-labeling has no effect on acceptance activity of tRNA$^{Met}_{f_1}$ as shown by Hara et al. (1970) and confirmed in the present study. It is difficult to ascertain whether the lowered acceptance activity of tRNA$^{Met}_{f_3}$ relative to tRNA$^{Met}_{f_1}$ is real because the difference is not greatly in excess of experimental error. However, there is no doubt that spin-labeling tRNA$^{Met}_{f_3}$ leads to a loss of 60% acceptor activity. Thus, the structure of SL-tRNA$^{Met}_{f_3}$, which lacks two tertiary base pairs found in native tRNA$^{Met}_{f_1}$, considerably reduces acceptance activity relative to either species

[4] The peak labeled g in the difference spectrum of native tRNA$^{Met}_{f_1}$ and tRNA$^{Met}_{f_3}$ (Figure 3A) may not be identical with g in the spin-labeled difference spectra (Figure 6), since the chemical shift of the former is about 0.2 ppm below the latter.

with only one of the tertiary base pairs lacking, i.e., SL-$tRNA^{Met}_{f_1}$ and native $tRNA^{Met}_{f_3}$.

The rate of aminoacylation reaction catalyzed by the synthetase from *E. coli* is an even more sensitive criterion of the structural differences between $tRNA^{Met}_{f_1}$ and $tRNA^{Met}_{f_3}$ than their respective acceptance activities. Differences in initial rates between $tRNA^{Met}_{f_1}$ and $tRNA^{Met}_{f_3}$ are much greater at low Mg^{2+} concentrations consistent with greater structural differences between the two. Under these conditions, $tRNA^{Met}_{f_1}$ is a better substrate than $tRNA^{Met}_{f_3}$. The differences that remain at high Mg^{2+} seem to favor $tRNA^{Met}_{f_3}$, since at high Mg^{2+} concentrations (cf. Figure 7), $tRNA^{Met}_{f_3}$ reacts more rapidly than $tRNA^{Met}_{f_1}$. At a Mg^{2+} concentration of 5.5 mM where native $tRNA^{Met}_{f_1}$ has an initial velocity of about 75% of native $tRNA^{Met}_{f_3}$, the spin-labeled modification of the latter yields only ~43% of the rate. It would seem that in the interaction between tRNA and the enzyme, Mg^{2+} can overcome the structural disorder introduced by lack of the G23-m^7G47 bond, but again cannot overcome the effect of the two missing bonds in spin-labeled $tRNA^{Met}_{f_3}$.

Acknowledgments

The authors express their thanks to A. Hu for her excellent technical assistance.

References

Clark, B. F. C. (1975), *Biochem. Soc. Trans. 3,* 645–649.

Crothers, D. M., Cole, P. E., Hilbers, C. W., and Shulman, R. G. (1974), *J. Mol. Biol. 87,* 63–88.

Daniel, W. E., Jr., and Cohn, M. (1975), *Proc. Natl. Acad. Sci. U.S.A. 72,* 2582–2586.

Daniel, W. E., Jr., Morrisett, J. D., Harrison, J. H., Dearman, H. H., and Hiskey, R. G. (1973), *Biochemistry 12,* 4918–4923.

Delaney, P., Bierbaum, J., and Ofengand, J. (1974), *Arch. Biophys. Biochem. 161,* 260–267.

Egan, B. Z., Weiss, J. F., and Kelmers, A. D. (1973), *Biochem. Biophys. Res. Commun. 55,* 320–327.

Favre, A., Michelson, A. M. and Yaniv, A. (1971), *J. Mol. Biol. 58,* 367–369.

Hara, H., Horiuichi, T., Saneyoshi, M., and Nishimura, S. (1970), *Biochem. Biophys. Res. Commun. 38,* 305–311.

Kallenbach, N. R., Daniel, W. E., Jr., and Kaminker, M. A. (1976), *Biochemistry 15,* 1218–1224.

Kan, L. S., Ts'o, P. O. P.-, Haar, F. v. d., Sprinzl, M., and Cramer, F. (1974), *Biochem. Biophys. Res. Commun. 59,* 22–29.

Kim, S. H., Sussman, J. L., Suddath, F. L., Quigley, G. J., McPherson, A., Wang, A. H. J., Seeman, N. C., and Rich, A. (1974), *Proc. Natl. Acad. Sci. U.S.A. 71,* 4970–4974.

Kornberg, R. D., and McConnell, H. M. (1971), *Biochemistry 10,* 1111–1120.

Ladner, J. E., Jack, A., Robertus, J. D., Brown, R. S., Rhodes, D., Clark, B. F. C., and Klug, A. (1975), *Proc. Natl. Acad. Sci. U.S.A. 72,* 4414–4418.

Lawrence, F., Blanquet, S., Poiret, M., Robert-Gero, M., and Waller, J.-P. (1973), *Eur. J. Biochem. 36,* 234–243.

Reid, B. R., and Robillard, G. T. (1975) *Nature (London) 257,* 287–291.

Robertus, J. D., Ladner, J. E., Finch, J. T., Rhodes, D., Brown, R. S., Clark, B. F. C., and Klug, A. (1974a), *Nature (London) 250,* 546–551.

Robertus, J. D., Ladner, J. E., Finch, J. T., Rhodes, D., Brown, R. S., Clark, B. F. C., and Klug, A. (1974b), *Nucleic Acids Res. 1,* 927–932.

Rozantsev, E. G., and Golubev, V. A. (1966), *Izv. Akad. Nauk Uzb. SSR, Ser. Khim. Nauk.* 891–895.

Roy, K. L., Bloom, A., and Söll, D. (1971), *Procedures Nucleic Acids Res. 2,* 524–541.

Seno, T., Kobayashi, M., and Nishimura, S. (1968), *Biochim. Biophys. Acta 169,* 80–94.

Shulman, R. G., Hilbers, C. W., Kearns, D. R., Reid, B. R., and Wong, Y. P. (1973), *J. Mol. Biol. 78,* 57–69.